ICIC Express Letters
Volume **17**, Number **9**, September **2023**

ICIC International ©2023 ISSN 1881-803X
pp. **967–978**

FUZZY LOGIC CONTROLLER FOR STABILIZING THE ROLLING MOVEMENT OF UAV BICOPTER

Fahmizal[1,2], Hanung Adi Nugroho[1,*], Adha Imam Cahyadi[1] and Igi Ardiyanto[1]

[1]Department of Electrical and Information Engineering
Engineering Faculty
Universitas Gadjah Mada
Kompleks Grafika, Yogyakarta 55281, Indonesia
{ fahmizal; adha.imam; igi }@ugm.ac.id
*Corresponding author: adinugroho@ugm.ac.id

[2]Department of Electrical Engineering and Informatics
Vocational College
Universitas Gadjah Mada
Kompleks Sekip, Yogyakarta 55281, Indonesia

Received September 2022; accepted December 2022

Abstract. *This paper describes the design of a fuzzy logic controller (FLC) for stabilizing the rolling motion of an unmanned aerial vehicle (UAV) Bicopter. Rolling motion control is part of the inner loop (attitude) control in UAV Bicopter, which is very important to control for achieving rapid settling time and stability. The Bicopter is a nonlinear, unstable, underactuated system and hard to model clearly in mathematics. In order to stabilize the rolling motion of a UAV Bicopter, this research proposes an embedded FLC. The developed FLC uses the Mamdani approach and varied rule base. The UAV Bicopter was placed on a test bed with a Teensy 3.6 microcontroller to validate our approach. The results of the experiments and tests were presented to demonstrate the proposed controller's validity.*

Keywords: UAV Bicopter, Fuzzy logic control, Attitude control, Rolling control

1. **Introduction.** In recent years, numerous studies have been conducted on unmanned aircraft, also known as unmanned aerial vehicles (UAVs). UAVs have a rich development history over the last two to three decades. There are currently two main types of small unmanned aerial vehicle platforms: fixed-wing and vertical takeoff and landing (VTOL). Each variety possesses unique strengths and limits, including flexibility, carrying capacity, and durability. Researchers are striving to develop a UAV that is simple to operate [1-3], energy efficient [4-6], has a larger payload capacity [7-9], and can travel over enormous distances.

Researchers who combine the benefits of fixed-wing and VTOL have developed the hybrid UAV. In general, hybrid UAVs are classified as either convertiplanes or tail-sitters. The convertiplane is a hybrid aircraft that takes off, hovers, and lands using a fixed horizontal fuselage reference line (the main fuselage configuration does not change during flight). Four sub-types of convertible UAVs are distinguished: 1) tilt-rotor [10,11], 2) tilt-wing [12,13], 3) rotor-wing [14,15], and 4) dual-system [16,17]. The tilt-rotor UAV (TRUAV) has several rotors mounted on an inclined shaft. During the hover-to-cruise transition, some or all of the rotors tilt toward the direction of flight to give the aircraft forward speed until cruise flight is achieved. Furthermore, TRUAV is categorized into three types [18], namely 1) bi-tilt rotor, 2) tri-tilt rotor, and 3) quad-tilt rotor.

DOI: 10.24507/icicel.17.09.967

In this study, we selected the TRUAV type with a bi-tilt rotor, also known as the UAV Bicopter. The benefit of this type of Bicopter is that it may be utilized for exploration flights in indoor applications or in narrow spaces, such as going through a house's door or window. Due to the reduced size, the required power consumption is likewise reduced. In addition, there are fewer sets of actuators in comparison to quadrotor and multirotor UAVs.

Bicopter may fly similar to other rotorcraft. The roll, pitch, and yaw torque necessary to regulate the Bicopter's attitude are derived from the difference in rotor speed and angle. Attitude control is a system that controls the orientation attitude of the Bicopter; hence its response speed is crucial. The Bicopter system's inner loop control includes attitude control in the form of rolling, pitching, and yawing movement regulation. To support the translational motion system as the outer loop, the three motion systems must have a rapid settling time.

Several researchers have carried out the design of Bicopter attitude control. Blouin and Lanteigne [19] described the use of oblique active tilting (OAT), which allows a faster pitch response due to the effects of gyroscopic torque. This study provides general guidelines for designing a Bicopter with OAT configuration using proportional-derivative (PD) control and lead controller. The simulation results in this study showed that the lead controller control produces a faster and better stability response compared to the PD control.

Furthermore, Zhang et al. [20] conducted a study related to the UAV Bicopter by discussing the basis of movement and designing the stability of the attitude. The first step in this research is to model the dynamics and simulate them using proportional-derivative-integrative (PID) control. Furthermore, a flight test was carried out to check the stability of the attitude using a tracking curve trajectory. In addition, a similar study was also conducted by Hrečko et al. [21] describing the implementation of N-PID control. The main difference in this study's type of PID control lies in the output structure of the nonlinear process placed after the PID controller itself. Papachristos et al. [22] from the University of Patras in Greece also conducted research related to PID control. This work discusses the nonlinear Bicopter model and linearization processes used to execute PID control in a simulation by measuring the position of the system's root locus after PID control has been applied. This study employs an experimental process for fine-tuning PID control parameters during the implementation phase.

The Bicopter is a nonlinear, unstable, and under-actuated system, which means that the system on the Bicopter has four control input signals to control six degrees of freedom of movement. Designing a controller can be obtained by knowing the system's characteristic equation (mathematical model) that characterizes the system's behavior. This equation is typically modeled as a linear equation that can be solved by a linear controller, such as the linear state space control theory. However, in actual conditions, the system encountered is generally nonlinear. However, there have been linearization methods, which convert nonlinear equations into linear equations and then try to solve them. Unfortunately, the linearization method is very limited to certain areas.

In intelligent control areas, many researchers demonstrated that the fuzzy logic controller (FLC) theory could be used to overcome the attitude problem in UAVs [23-27]. From the literature review, the Bicopter attitude control is generally controlled using a PID controller. However, this paper discusses maintaining the attitude of the UAV Bicopter in rolling motion by applying FLC. This paper contributes to developing embedded FLC to stabilize the rolling motion of the Bicopter in the test bed. The remainder of this paper is organized as follows. In Section 2, the mechanical and electronics of Bicopter are proposed. Section 3 elaborates the control system architectures especially on fuzzy system for controlling attitude of Bicopter. Section 4 presents several simulation results which show the effectiveness and merit of the proposed methods. Section 5 concludes the paper with remarks and suggestions for future works.

2. Materials and Methods.

2.1. Mechanical and electronics Bicopter. The Bicopter is constructed with two driving rotors and two servo motors for tilting the two rotors in opposite directions. Figure 1 shows the right rotor thrust (F_R) and left rotor thrust (F_L) created by the rotor, propeller, and their components in the x and z axes. By altering the magnitude of the rotor thrusts F_R and F_L, the rolling movement may be adjusted. This research develops the platform using Autodesk Inventor Student version and UP2 3D printer [28].

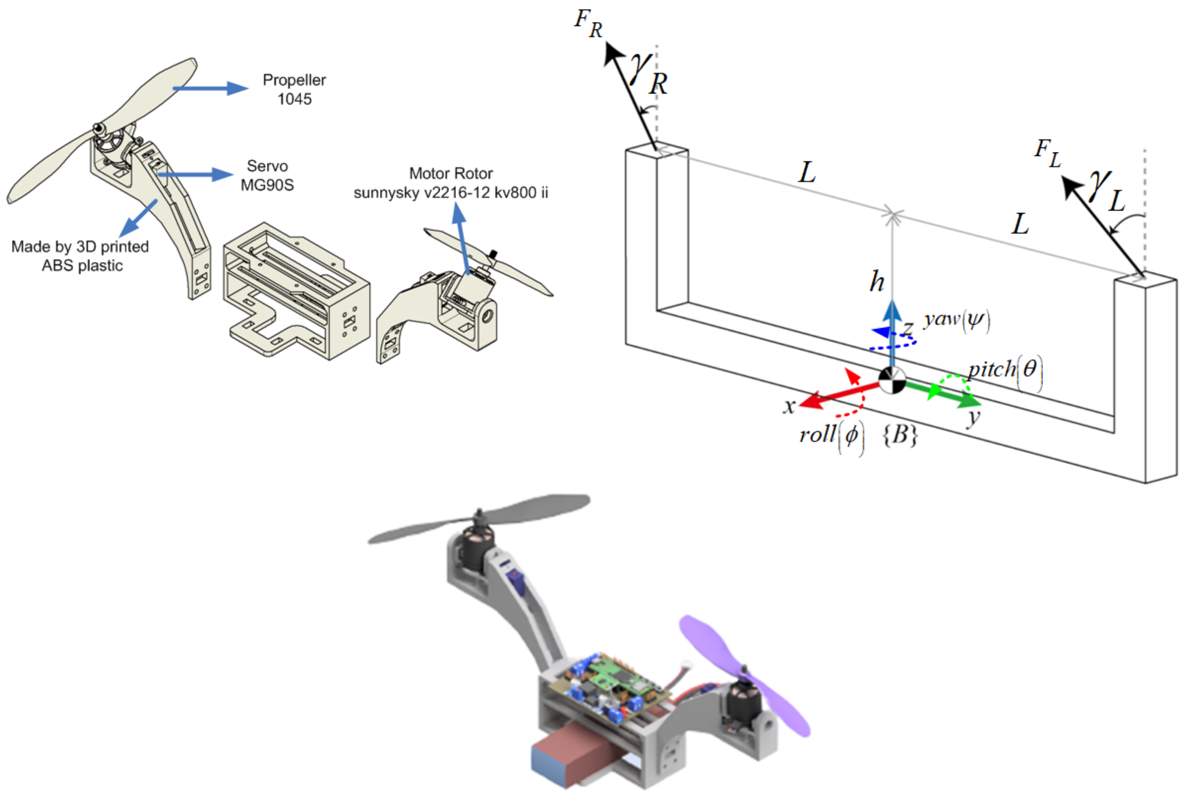

FIGURE 1. Mechanical design of Bicopter

Teensy 3.6 serves as the primary Microcontroller in the Bicopter electronics system. There are two MG90S servo motors with one motor for each of the left and right rotors and one MPU 6050 IMU sensor [29]. The electronic system is also coupled with a personal computer (PC) via serial communication with the Graphical User Interface (GUI) to automatically show sensor reading conditions in real time. Figure 2 represents the results of the Printed Circuit Board (PCB) design for the UAV Bicopter electronic system. This PCB is also known as the Bicopter's flight controller.

2.2. Fuzzy logic control. Professor Lutfi A. Zadeh, a computer science researcher from California University, created fuzzy logic in 1965. Professor Zadeh assumes that true and false logic (firm logic) cannot reflect every human concept; hence, he develops fuzzy logic to describe every scenario or human thought [30]. The membership of elements in a set is what differentiates firm logic from fuzzy logic.

This paper employs a fuzzy inference system based on the Mamdani technique, also known as the min-max approach. Mamdani and Assilian introduced this approach in 1975 [31]. To get fuzzy logic output, it takes four stages, as follows.

1) Fuzzification converts discrete values into a fuzzy set's degree of membership for linguistic terms.

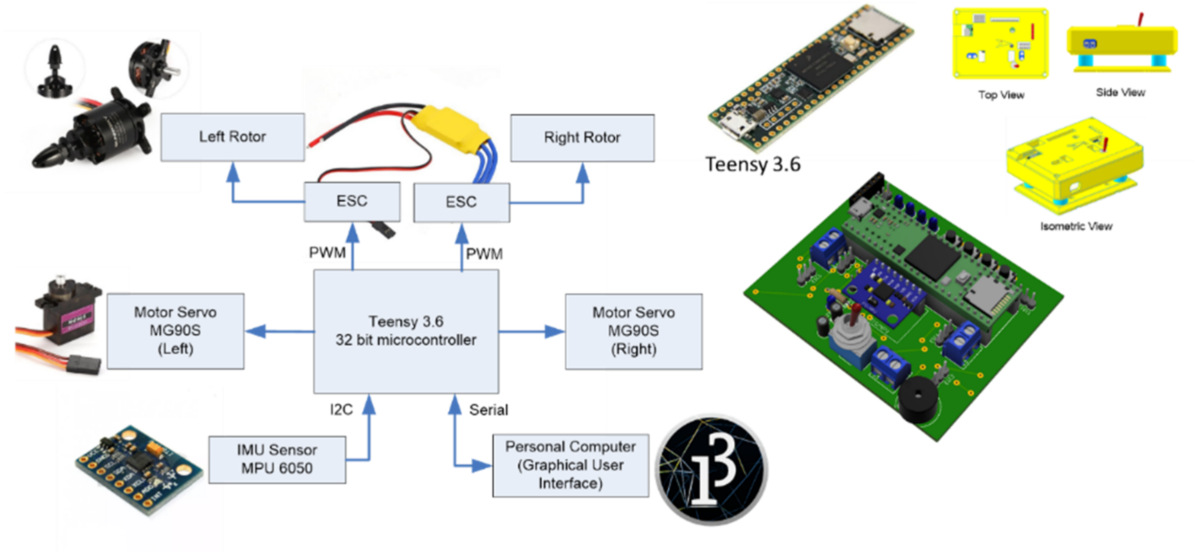

FIGURE 2. Electronic design of Bicopter

2) The fuzzy implication is to analyze each rule's consequence. After the inputs have been fuzzified, fuzzy logic control is able to determine the extent to which a portion of the antecedent rule is met. The equation of the Mamdani approach to validating the fuzzy implication can be found in Equation (1).

$$\mu_y(k) = \max\left[\min\left\{\mu_u(k), \mu_r(k)(error(i), derror(i))\right\}\right] \tag{1}$$

3) Creating the rules for a fuzzy control system is frequently the most challenging design stage. It is normally necessary to have some expert knowledge of plant dynamics. In fuzzy system inference, three approaches are utilized: max, additive, and probabilistic OR (union). Using the max technique, the fuzzy set solution can be obtained by first determining the maximum rule value, then modifying the fuzzy area, and finally applying the modified fuzzy region to the output using the OR operator.
4) Weight average (WA) was proposed for the defuzzification stage. Equation (2) describes the WA computation utilizing the three singletons membership function.

$$y = \frac{\mu(k1) \times k1 + \mu(k2) \times k2 + \mu(k3) \times k3}{\mu(k1) + \mu(k2) + \mu(k3)} \tag{2}$$

3. Control Design.

3.1. Attitude control.
One of the problems with Bicopter is the flight attitude control. This control aims to stabilize the Bicopter's orientation position. Attitude control (or inner loop), which regulates the Bicopter's orientation through rotational movement. As the inner loop of the Bicopter system, the rotating motion system must support the translational motion system with a fast settling time. Figure 3 shows the block diagram of a closed loop control system for the Bicopter's attitude stability. It is evident from this block diagram that there are four closed loops. The first loop is for the Bicopter's altitude control, while the second, third, and fourth loops are for the Bicopter's attitude control on the orientation of roll (ϕ), pitch (θ) and yaw (ψ).

3.2. Fuzzy scheme control.
A fuzzy logic controller (FLC) is part of an effective knowledge base system controlling a very complex system to model clearly, such as a Bicopter. In this section, we described the FLC for controlling the attitude of the Bicopter under rolling movement conditions. A block diagram of the roll control system is shown in Figure 4. By giving an input reference, set point (SP) signal, in the form of a Bicopter roll angle of 0 degrees then, the deviation of the current roll angle (ϕ) to the reference roll

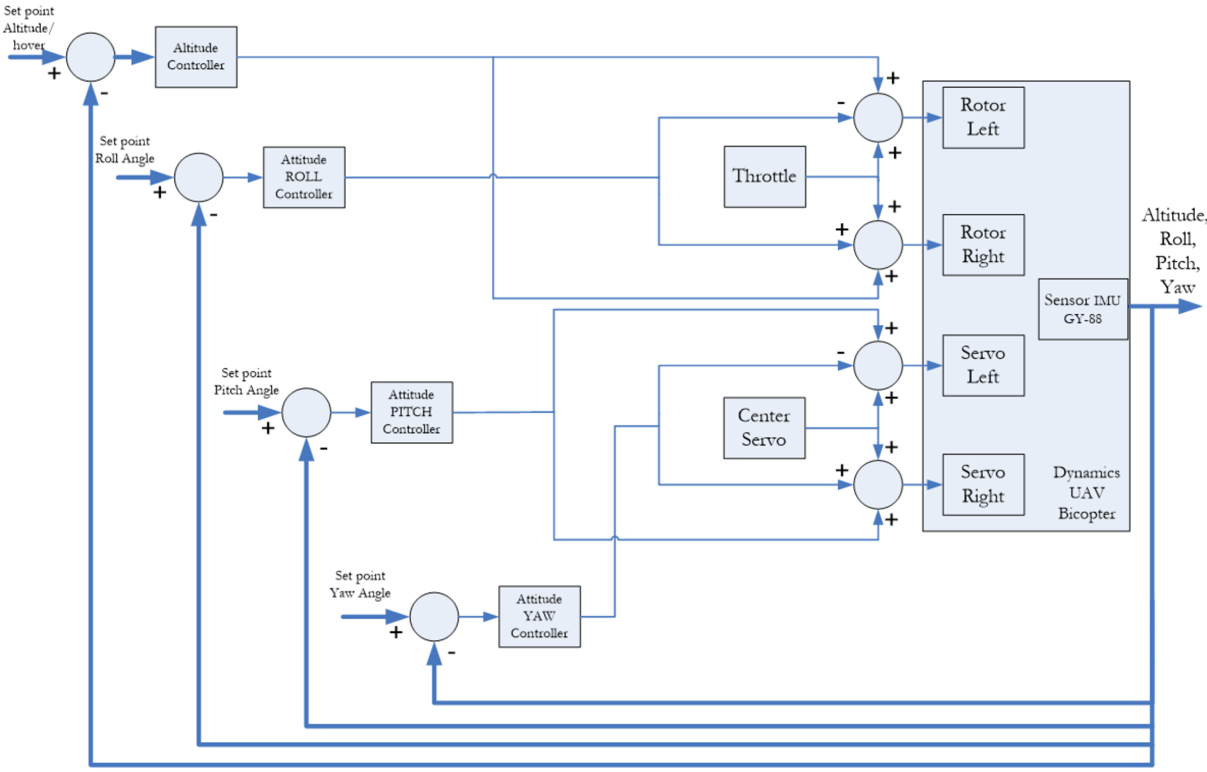

FIGURE 3. Block diagram of a closed loop control system for the Bicopter

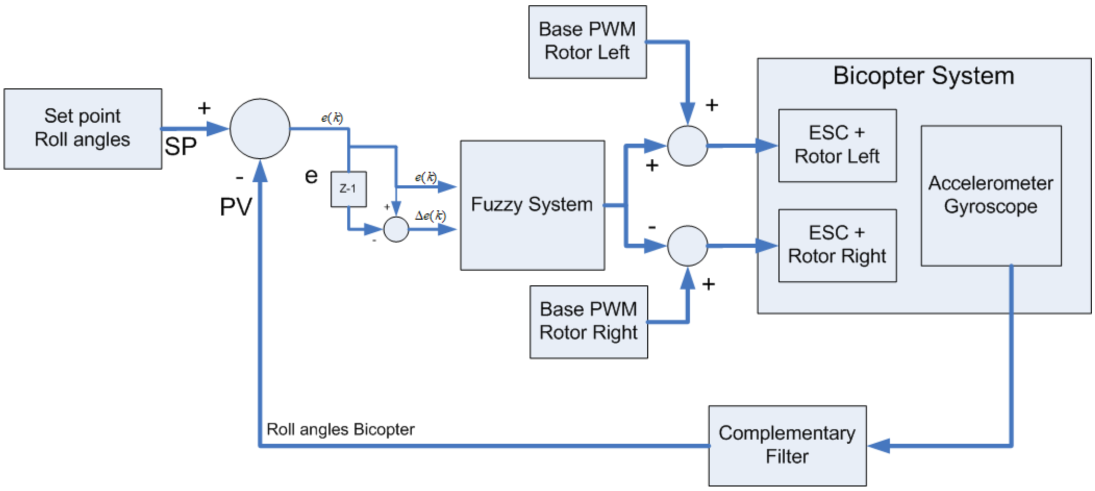

FIGURE 4. Feedback control scheme of stabilizing rolling movement Bicopter using fuzzy logic controller

angle (ϕ_r) is defined as error system in Equation (3). Moreover, if we know the error (e), we may calculate the delta error (Δe) as indicated in Equation (4) where $\dot{e}$ is last error.

$$e = \phi - \phi_r \tag{3}$$

$$\Delta e = e - \dot{e} \tag{4}$$

The error and delta error values are then processed using the embedded FLC method into the microcontroller (Teensy 3.6). The output of this FLC stage is shown in Figure 5. The FLC stages start with the fuzzification process, continue with the inference process, and end with the defuzzification process. The results of this FLC process will be added up with the reference base pulse value for the left rotor and reduced by the reference base pulse value for the right rotor. An inertia measurement unit (IMU) sensor from the MPU

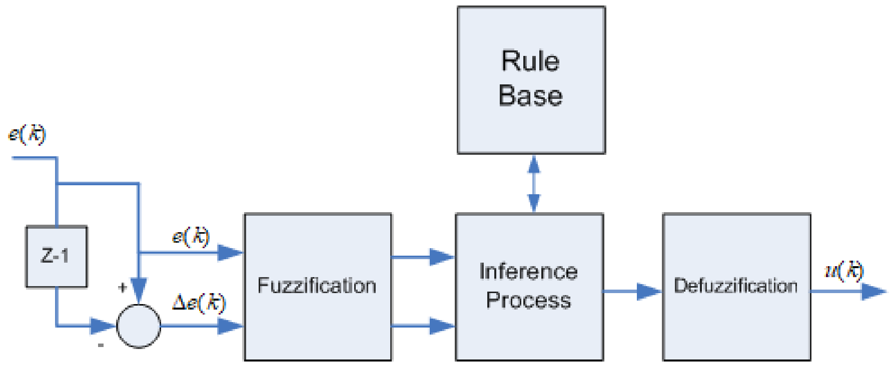

Figure 5. Block diagram for fuzzy logic system

6050 series is utilized to obtain a readout of the roll angle Bicopter. The angle reading results from the IMU sensor will be greatly influenced by noise in the form of vibration, so a complementary filter (CF) is needed to maintain the sensor reading results IMU from noise.

As shown in Figure 5, once the error and delta error have been computed according to Equation (3) and Equation (4), these values are used as input variables for the FLC design. Using the triangle membership function, we developed four types of fuzzification processes for error and delta error, as shown in Figure 6 and Figure 7, respectively. NB, ZE, and PB represent the error and delta error membership functions with the rule base I (3×3) in Table 1. Error and delta error with the rule base II (5×5) in Table 2 are denoted by NB, NS, ZE, PS, and PB, respectively, for membership functions. Additionally, NB, NM, NS, ZE, PS, PM, and PB represent the membership function of error and delta error with the rule base III (7×7) presented in Table 3. Finally, the error and delta error membership functions with the rule base IV (9×9) in Table 4 are denoted by NVB, NB, NM, NS, ZE, PS, PM, PB, PVB. All membership abbreviations are described in Table 5.

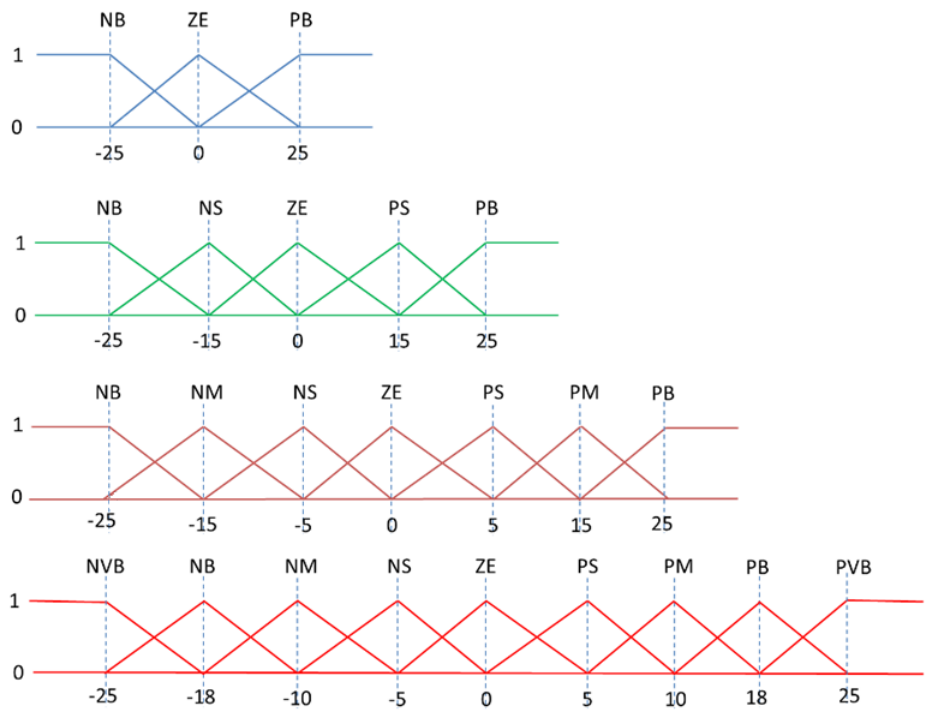

Figure 6. Four types of error membership functions

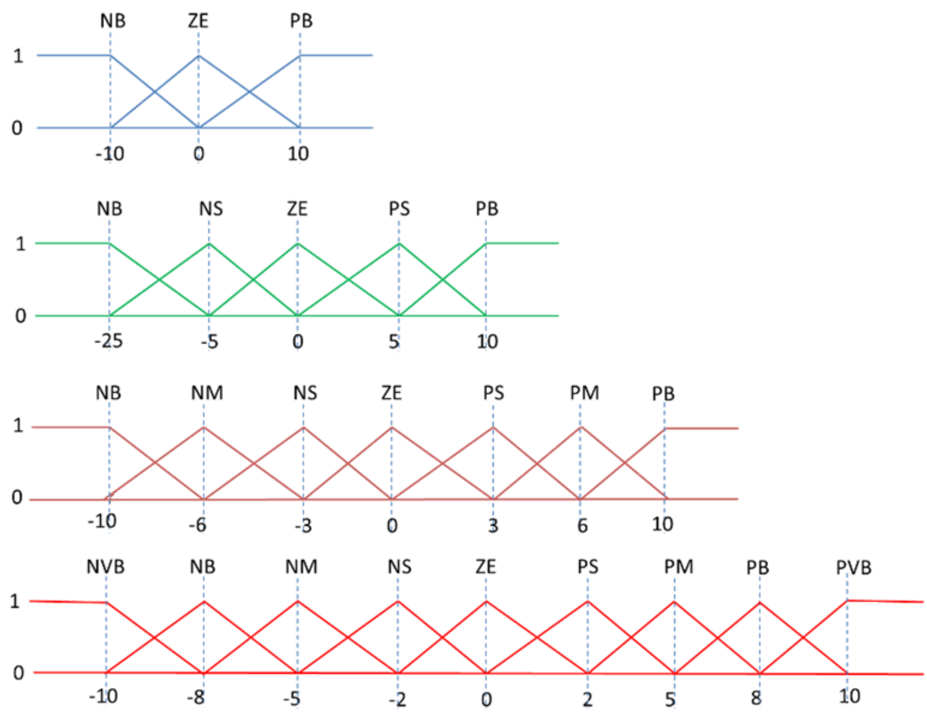

FIGURE 7. Four types of delta error membership functions

TABLE 1. Rule base I (3 × 3)

		error		
		NB	ZE	PB
derror	NB	NB	NS	ZE
	ZE	NS	ZE	PS
	PB	ZE	PS	PB

TABLE 2. Rule base II (5 × 5)

		error				
		NB	NS	ZE	PS	PB
derror	NB	NB	NB	NS	NS	ZE
	NS	NB	NS	ZE	ZE	PS
	ZE	NS	ZE	ZE	ZE	PS
	PS	NS	ZE	ZE	PS	PB
	PB	ZE	PS	PS	PB	PB

TABLE 3. Rule base III (7 × 7)

		error						
		NB	NM	NS	ZE	PS	PM	PB
derror	NB	NB	NM	NM	NS	NS	NS	ZE
	NM	NM	NM	NS	NS	ZE	ZE	PS
	NS	NM	NS	NS	ZE	ZE	ZE	PS
	ZE	NS	NS	ZE	ZE	ZE	PS	PS
	PS	NS	ZE	ZE	ZE	PS	PS	PM
	PM	NS	ZE	ZE	PS	PS	PM	PM
	PB	ZE	PS	PS	PS	PM	PM	PB

TABLE 4. Rule base IV (9 × 9)

		error								
		NVB	NB	NM	NS	ZE	PS	PM	PB	PVB
derror	NVB	NVB	NVB	NB	NB	NM	NM	NS	NS	ZE
	NB	NVB	NB	NM	NM	NS	NS	ZE	ZE	PS
	NM	NB	NM	NM	NS	NS	ZE	ZE	ZE	PS
	NS	NB	NM	NS	NS	ZE	ZE	ZE	PS	PM
	ZE	NM	NS	NS	ZE	ZE	ZE	PS	PS	PM
	PS	NM	NS	ZE	ZE	ZE	PS	PS	PM	PB
	PM	NS	ZE	ZE	ZE	PS	PS	PM	PM	PB
	PB	NS	ZE	ZE	PS	PS	PM	PM	PB	PVB
	PVB	ZE	PS	PS	PM	PM	PB	PB	PVB	PVB

TABLE 5. Membership function abbreviations

Membership function	Stands for abbreviation
NVB	Negative very big
NB	Negative big
NM	Negative medium
NS	Negative small
ZE	Zero
PS	Positive small
PM	Posistive medium
PB	Positive big
PVB	Positive very big

After the rule base stage is completed, it is continued in the defuzzification process. The output from this step is then used to increase or decrease the rotational speed of the Bicopter's rotor and will affect the rolling (ϕ) movement of the Bicopter as described in Equation (5), where L is the horizontal distance of center of gravity (CoG) and the rotor center, C_T is the thrust coefficient, I_{xx} is the moment of inertia along the x-axis, Ω_L and Ω_R are the left rotor speed and the right rotor speed. Because there are four variations of the rule base design, the output at the defuzzification stage also has four variations of the singleton function, as shown in Figure 8.

$$\ddot{\phi} = \frac{L}{I_{xx}} C_T \left(\Omega_R^2 - \Omega_L^2\right) \tag{5}$$

4. **Results and Discussion.** In order to implement the proposed controller, embedded FLC was built into Teensy 3.6. The Bicopter is tested in a test bed to evaluate the performance of the proposed controller, as shown in Figure 9. In this experiment, the Bicopter was placed in a roll condition at an angle of −28 degrees. Figure 10 shows that the four experiments produced results when the rule base IV provided an excellent response performance. As shown in Table 6, when the rule base is 9 × 9, it can be represented with the minimum mean square error (MSE) result. In addition, the Bicopter experiment demonstrated promising results when disturbed, as illustrated in Figure 11. Furthermore, the 9 × 9 rule base can produce a good response when faced with a change in the reference point.

Figure 10(a) shows the response of the system by using the 3 × 3 inference rule base process. When evaluated on the test bed, the response to the Bicopter's roll angle movement exhibits oscillations with a root mean square error (RMSE) value of 4.8540. In addition,

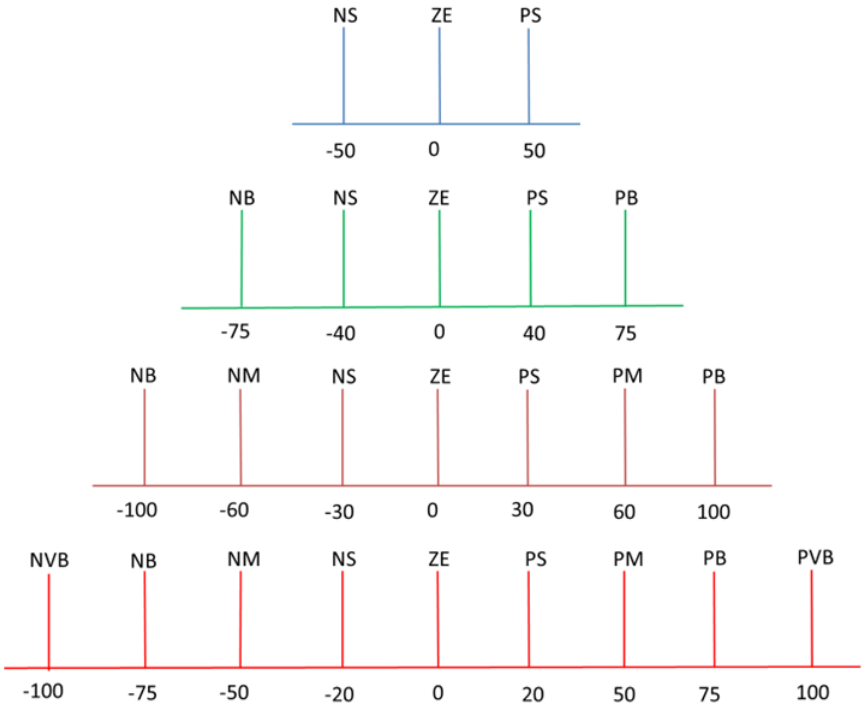

FIGURE 8. Four types of defuzzification using singleton functions

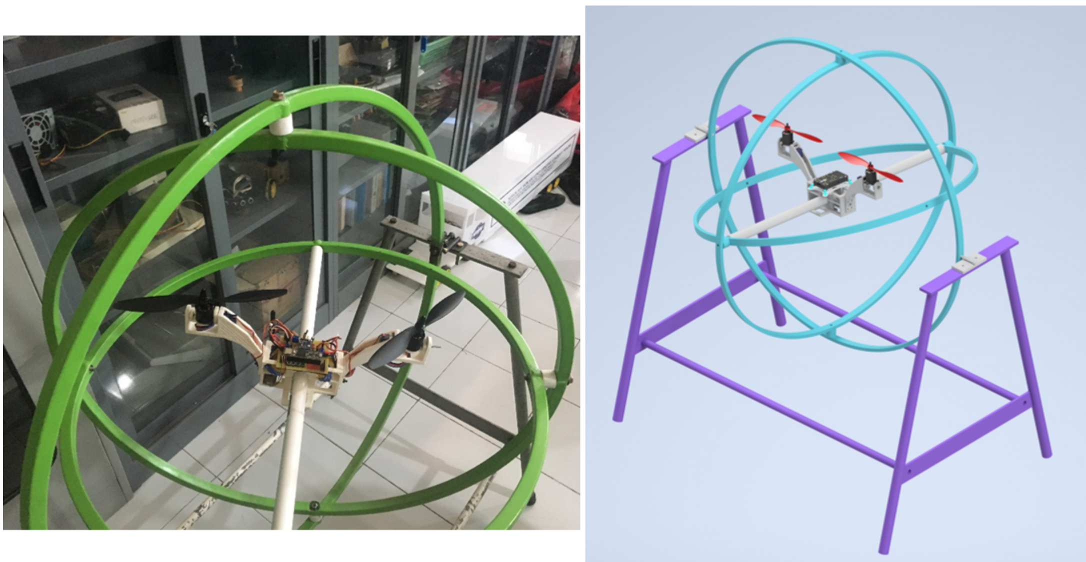

FIGURE 9. A test bed evaluating the Bicopter's performance

when the rule base for inference was set to 7×7, it saw an increase in stability along with a significant reduction in the RMSE, which brought it down to 4.0166. The best experimental results are obtained when the inference rules base is set at 9×9 as proven by the RMSE calculation results, which decrease to 3.9748. The experimental results using more rule base numbers show that the RMSE results will decrease, and the Bicopter system does not experience oscillations, as shown in Figure 10(d).

When employing the 9×9 rule base, it is also possible to examine the response of the system to disturbances as well as changes in the set point. Figure 11(a) shows that when the disturbance came at 5 seconds, the roll angle experienced an oscillation but was quickly damped down for around 1.5 seconds. Likewise, with the condition when changing the set point, when it is 3.8 seconds, the roll reference angle is at 10 degrees as shown in

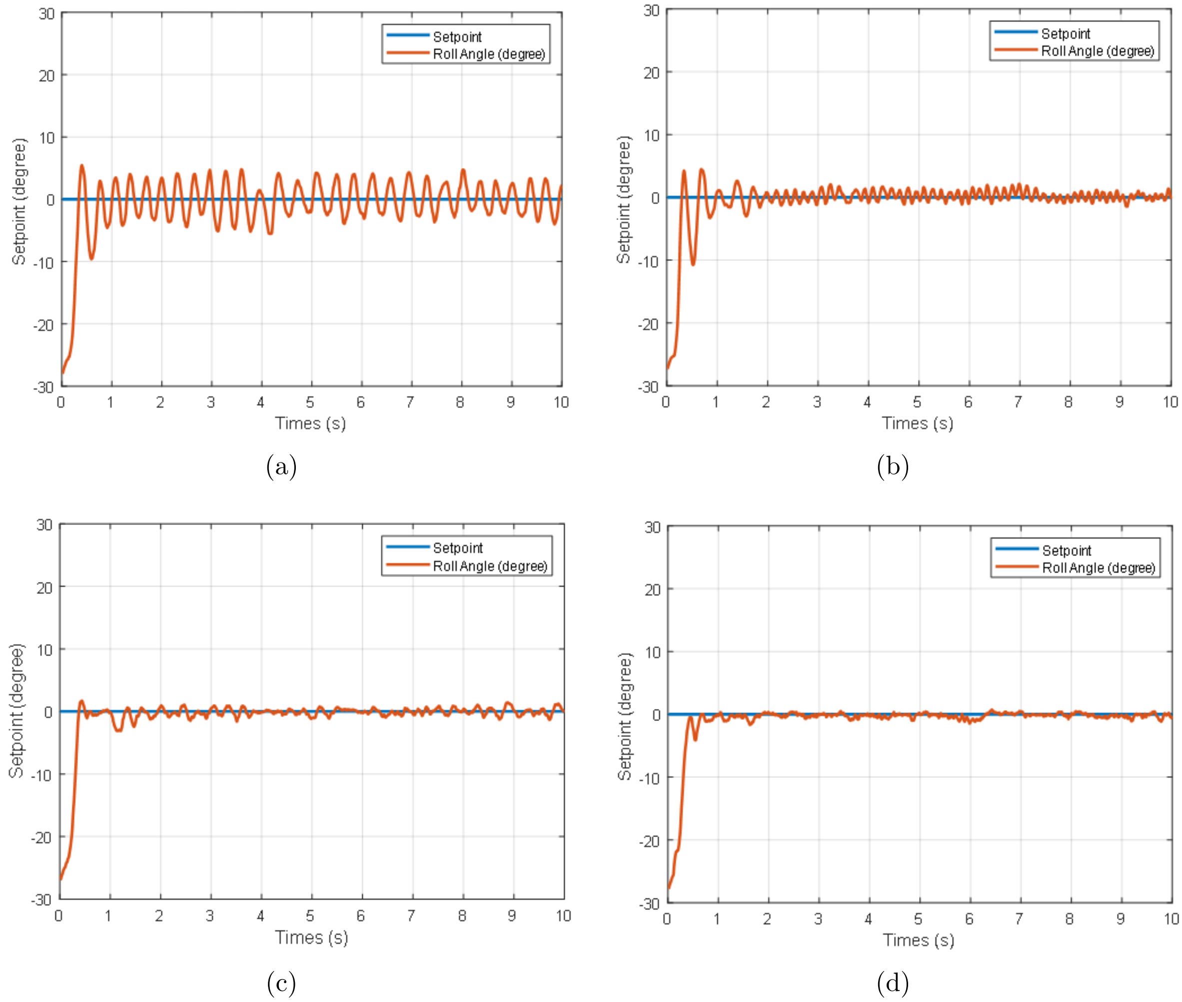

FIGURE 10. The rule based performance response for roll angle: (a) Rule base 3×3, (b) rule base 5×5, (c) rule base 7×7, and (d) rule base 9×9

TABLE 6. Mean square error (MSE) and root mean square error (RMSE) of rule based performance

Rule base type	MSE	RMSE
Rule base I (3×3)	23.5617	4.8540
Rule base II (5×5)	16.5812	4.0720
Rule base III (7×7)	16.1333	4.0166
Rule base IV (9×9)	15.7989	3.9748

Figure 11(b), and the roll angle response on the Bicopter achieves reference in less than 1 second. These results indicate that performance using the 9×9 rule base produces a good response.

5. **Conclusions.** This paper details the procedure followed in the development of FLC for the Bicopter's rolling motion stabilization. An embedded FLC with microcontroller Teensy 3.6 is responsible for the implementation. The findings from the rule base design indicated that an RMSE of 3.9748 was the best possible value for the 9×9 rule base. In addition to that, testing as well as the observation of disturbances was carried out.

This study still contains limitations because it has just discussed controlling the attitude of the Bicopter at roll angle, and it can still be developed for further research by adding dynamic angle movements from the Bicopter such as pitch and yaw angles. In addition,

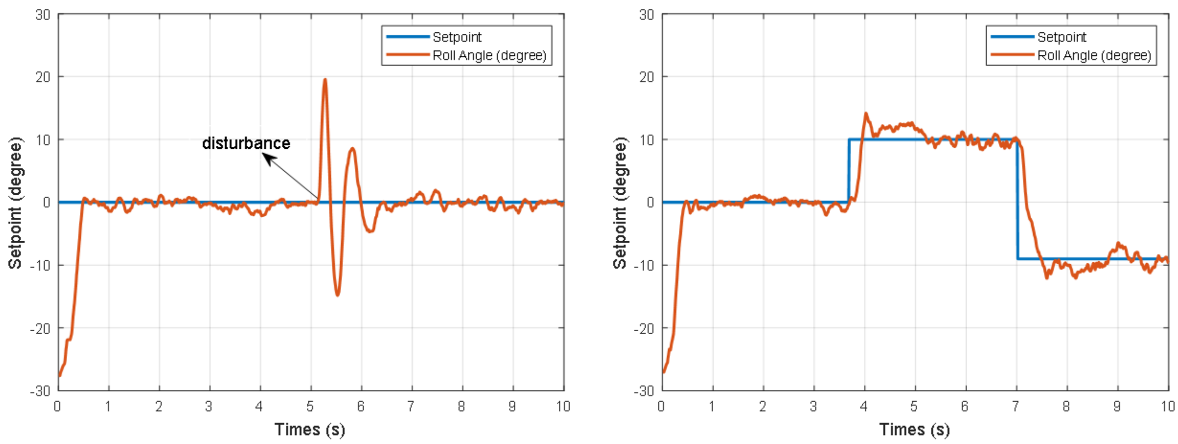

(a) (b)

Figure 11. The performance response using rule base 9×9 when (a) given disturbance and (b) the set point is changed

due to the non-linear character of the Bicopter, the non-linear controller type is a solution that has to be researched further.

Acknowledgment. The Postgraduate Domestic Education Scholarship (BPPDN) from the Indonesian Ministry of Research, Technology, and Higher Education provided funding for this study with contract number 2974/UN1.P.IV/KPT/DSDM/2019.

REFERENCES

[1] Q. Ali and S. Montenegro, Explicit model following distributed control scheme for formation flying of mini UAVs, *IEEE Access*, vol.4, pp.397-406, 2016.
[2] M. R. Cohen, K. Abdulrahim and J. R. Forbes, Finite-horizon LQR control of Quadrotors on $SE_2(3)$, *IEEE Robot. Autom. Lett.*, vol.5, no.4, pp.5748-5755, 2020.
[3] Y. Li, Q. Ding, S. Li and S. Valtchev, Optimal controller design for non-affine nonlinear power systems with static VAR compensators for hybrid UAVs, *Tsinghua Sci. Technol.*, vol.27, no.1, pp.196-206, 2021.
[4] S. Ahmed, M. Z. Chowdhury and Y. M. Jang, Energy-efficient UAV-to-user scheduling to maximize throughput in wireless networks, *IEEE Access*, vol.8, pp.21215-21225, 2020.
[5] Q. V. Do, Q.-V. Pham and W.-J. Hwang, Deep reinforcement learning for energy-efficient federated learning in UAV-enabled wireless powered networks, *IEEE Commun. Lett.*, vol.26, no.1, pp.99-103, 2021.
[6] Z. Yang, W. Xu and M. Shikh-Bahaei, Energy efficient UAV communication with energy harvesting, *IEEE Trans. Veh. Technol.*, vol.69, no.2, pp.1913-1927, 2019.
[7] M. Becker and D. Sheffler, Designing a high speed, stealthy, and payload-focused VTOL UAV, *IEEE Systems and Information Engineering Design Symposium (SIEDS)*, pp.176-180, 2016.
[8] T. Muskardin et al., A novel landing system to increase payload capacity and operational availability of high altitude long endurance UAVs, *J. Intell. Robot. Syst.*, vol.88, no.2, pp.597-618, 2017.
[9] W. Jin, J. Yang, Y. Fang and W. Feng, Research on application and deployment of UAV in emergency response, *IEEE 10th International Conference on Electronics Information and Emergency Communication (ICEIEC)*, pp.277-280, 2020.
[10] A. S. Saeed, A. B. Younes, C. Cai and G. Cai, A survey of hybrid unmanned aerial vehicles, *Prog. Aerosp. Sci.*, vol.98, pp.91-105, 2018.
[11] A. Vuruskan, B. Yuksek, U. Ozdemir, A. Yukselen and G. Inalhan, Dynamic modeling of a fixed-wing VTOL UAV, *IEEE 2014 International Conference on Unmanned Aircraft Systems (ICUAS)*, Orlando, FL, USA, pp.483-491, 2014.
[12] G. J. J. Ducard and M. Allenspach, Review of designs and flight control techniques of hybrid and convertible VTOL UAVs, *Aerosp. Sci. Technol.*, vol.118, 107035, 2021.
[13] E. Çetinsoy et al., Design and development of a tilt-wing UAV, *Turkish J. Electr. Eng. Comput. Sci.*, vol.19, no.5, pp.733-741, 2011.

[14] K. T. Oner, E. Çetinsoy, M. Unel, M. F. Akşit, I. Kandemir and K. Gülez, Dynamic model and control of a new quadrotor unmanned aerial vehicle with tilt-wing mechanism, *International Conference on Control, Automation, Robotics and Vision*, Paris, France, 2008.

[15] W. Sun, H. Wang and Z. J. Shang, Numerical study of interactive flow field for a canard rotor wing aircraft, *The 21st Australasian Fluid Mechanics Conference*, Adelaide, Australia, 2018.

[16] R. Park, *Arcturus UAV Upgrades the JUMP^{TM}15 VTOL UAV*, Airlines Aviat. Aerosp. Def., 2014.

[17] M. Hanel, M. Haimerl and T. Bienert, Flight control laws for the quadcruiser RPA, *Deutsche Gesellschaft für Luft-und Raumfahrt-Lilienthal-Oberth e.V.*, Bonn, DOI: 10.25967/480033, 2018.

[18] Z. Liu, Y. He, L. Yang and J. Han, Control techniques of tilt rotor unmanned aerial vehicle systems: A review, *Chinese J. Aeronaut.*, vol.30, no.1, pp.135-148, 2017.

[19] C. Blouin and E. Lanteigne, Pitch control of an oblique active tilting bi-rotor, *IEEE 2014 International Conference on Unmanned Aircraft Systems (ICUAS)*, Orlando, FL, USA, pp.791-799, 2014.

[20] Q. Zhang, Z. Liu, J. Zhao and S. Zhang, Modeling and attitude control of bi-copter, *IEEE/CSAA Int. Conf. Aircr. Util. Syst.*, pp.172-176, 2016.

[21] L. Hrečko, J. Slačka and M. Halás, Bicopter stabilization based on IMU sensors, *The 20th Int. Conf. Process Control*, pp.192-197, 2015.

[22] C. Papachristos, K. Alexis and A. Tzes, Design and experimental attitude control of an unmanned tilt-rotor aerial vehicle, *The 15th International Conference on Advanced Robotics (ICAR)*, pp.465-470, 2011.

[23] A. Al-Mahturi, F. Santoso, M. A. Garratt and S. G. Anavatti, Self-learning in aerial robotics using type-2 fuzzy systems: Case study in hovering quadrotor flight control, *IEEE Access*, vol.9, pp.119520-119532, 2021.

[24] V. P. Tran, F. Santoso, M. A. Garratt and I. R. Petersen, Distributed formation control using fuzzy self-tuning of strictly negative imaginary consensus controllers in aerial robotics, *IEEE/ASME Trans. Mechatronics*, vol.26, no.5, pp.2306-2315, 2020.

[25] H. K. Tran, J.-S. Chiou, N. T. Nam and V. Tuyen, Adaptive fuzzy control method for a single tilt tricopter, *IEEE Access*, vol.7, pp.161741-161747, 2019.

[26] E. Kayacan and R. Maslim, Type-2 fuzzy logic trajectory tracking control of quadrotor VTOL aircraft with elliptic membership functions, *IEEE/ASME Trans. Mechatronics*, vol.22, no.1, pp.339-348, 2016.

[27] Q. Chen, M. Tao, X. He and L. Tao, Fuzzy adaptive nonsingular fixed-time attitude tracking control of quadrotor UAVs, *IEEE Trans. Aerosp. Electron. Syst.*, vol.57, no.5, pp.2864-2877, 2021.

[28] T. L. Khuong, Z. Gang, M. Farid and R. Yu, Izod impact strength of acrylonitrile butadiene styrene (ABS) matetials after used in UP2! 3D-printer, *Applied Mechanics and Materials*, vol.713, pp.2737-2740, 2015.

[29] D. S. Fedorov, A. Y. Ivoilov, V. A. Zhmud and V. G. Trubin, Using of measuring system MPU6050 for the determination of the angular velocities and linear accelerations, *Autom. Softw. Enginery*, vol.11, no.1, pp.75-80, 2015.

[30] L. A. Zadeh, The birth and evolution of fuzzy logic, *Int. J. Gen. Syst.*, vol.17, nos.2-3, pp.95-105, 1990.

[31] E. H. Mamdani and S. Assilian, An experiment in linguistic synthesis with a fuzzy logic controller, *Int. J. Man. Mach. Stud.*, vol.7, no.1, pp.1-13, 1975.